

# Charged-Higgs-boson effect in $B_d^0$ - $\bar{B}_d^0$ mixing, $K \rightarrow \pi \nu \bar{\nu}$ decay, and rare decays of $B$ mesons

C. Q. Geng and John N. Ng

Theory Group, TRIUMF 4004 Wesbrook Mall, Vancouver, British Columbia, Canada V6T 2A3

(Received 31 May 1988)

Extensions of the standard model containing two Higgs-boson doublets leads to the existence of charged Higgs bosons which can be important in rare meson decays, such as  $K \rightarrow \pi \nu \bar{\nu}$ ,  $B_d \rightarrow X_s \nu \bar{\nu}$ , and  $B_d \rightarrow X_s \gamma$ . We analyze these in the minimal two Higgs-boson doublets with the constraint placed on the charged-Higgs-boson mass, the  $t$ -quark mass, and the ratio of the vacuum expectation values of the two doublets by  $B_d^0$ - $\bar{B}_d^0$  mixing. An enhancement factor of  $\sim 1.5$  over the prediction of the standard model is obtained for the branching ratio of  $K \rightarrow \pi \nu \bar{\nu}$ .

## I. INTRODUCTION

It is now generally accepted that the standard model (SM) is a good description of physics below the Fermi scale. However, its use of the Higgs mechanism to generate fermion and gauge bosons is *ad hoc* and we lack a physical understanding of how this works. Unhindered by this deficiency in understanding, and motivated by a desire to unify the strong and electroweak interactions within a grand unified theory, many theorists believe that the elementary scalar Higgs doublet of the standard model is only part of a much richer structure. This is especially true of supersymmetric unification theories. In the supersymmetric version of the standard model at least two Higgs doublets are necessary. Even without embedding the standard model within grand unified theories it is well known that a minimum of two Higgs doublets are required to solve the strong  $CP$  problem<sup>1</sup> of the standard model with the Peccei-Quinn mechanism.<sup>2</sup>

With two Higgs doublets, after spontaneous symmetry breaking (SSB), the spectrum of physical spin-0 bosons consists of two charged ones and three neutral ones. The discovery of the charged Higgs boson will be clear evidence of physics beyond the standard model. Certainly, a complete determination of the Higgs-boson spectrum and their couplings to fermion and gauge bosons is necessary for a better understanding of this mysterious SSB mechanism. The search of such states is very high on the list of experiments at future colliders such as the Superconducting Super Collider<sup>3</sup> (SSC). In the immediate future, the SLC and CERN LEP will be able to probe the existence of both charged and neutral Higgs bosons up to masses  $\leq \frac{1}{2}M_Z$ . It is also important to look for virtual effects of this extended Higgs structure in rare decays. This is not only complementary to direct Higgs-boson searches but can also provide important guides to these searches.

In this paper we examine the possible role charged Higgs bosons may play in rare decays of mesons. In particular, we focus on the following rare decays:

$$K^\pm \rightarrow \pi^\pm \nu \bar{\nu}, \quad (1.1)$$

$$B \rightarrow X_s \nu \bar{\nu}, \quad (1.2)$$

and

$$B \rightarrow X_s \gamma, \quad (1.3)$$

where  $X_s$  denotes inclusive final states involving strangeness. Immediate experimental interest is focused on (1.1) where data are now being collected.<sup>4</sup> In studying these reactions we use the simplest extension of SM by adding just one more Higgs doublet. The two Higgs doublets are denoted by  $\phi_1$  and  $\phi_2$ . Their couplings to fermions are such that  $\phi_1$  couples to  $u$ -type quarks and  $\phi_2$  couples to  $d$ -type quarks and leptons. This arrangement avoids flavor-changing neutral currents. Furthermore, we have made no attempt to include right-handed neutrinos; hence all neutrinos are massless in our calculations. Henceforth, we shall refer to this as the minimal charged-Higgs-boson (MCH) model. The theoretical motivation of examining the reactions (1.1)–(1.3) and not others is that the neutral Higgs bosons do not participate and we are free of the uncertainties involving them. In particular, the details of the Higgs potential will not be important to us.

In Sec. II we give details of the Lagrangian involving charged Higgs bosons. The constraint on the  $t$ -quark mass  $m_t$ , the charged-Higgs-boson mass  $M_H$ , and the ratio  $\xi \equiv v_2/v_1$ , where  $v_1$  and  $v_2$  are the vacuum expectation values of  $\phi_1$  and  $\phi_2$ , respectively, are obtained from  $B^0$ - $\bar{B}^0$  mixing. As expected, this mixing is sensitive to the parameters of the MCH model. This is used as input to calculate the branching ratio of reactions (1.1)–(1.3). Charged-Higgs-boson effects in (1.3) were calculated in Ref. 5. We use their results to compare with (1.1) and (1.2) and see that they behave as a function of  $m_t$  for fixed  $\xi$ . Section III discusses implications of our results. Throughout we assume that there are only three quark-lepton families. Adding more families will introduce too many unknown parameters and a meaningful analysis would be difficult to achieve.

## II. CALCULATION OF BOX DIAGRAM AND RARE DECAYS

The  $SU(2) \times U(1)$ -invariant Lagrangian<sup>6</sup> involving the two Higgs-boson doublets

$$\phi_1 = \begin{pmatrix} \phi_1^+ \\ \phi_1^0 \end{pmatrix} \quad \text{and} \quad \phi_2 = \begin{pmatrix} \phi_2^+ \\ \phi_2^0 \end{pmatrix}$$

is given by

$$\mathcal{L} = |D_\mu \phi_1|^2 + |D_\mu \phi_2|^2 + \mathcal{L}_Y - V(\phi_1, \phi_2), \quad (2.1)$$

where  $D_\mu$  is the covariant derivative. The specific form of the Higgs potential  $V(\phi_1, \phi_2)$  is not important to us and we will not display it. The Yukawa interactions  $\mathcal{L}_Y$  are explicitly given as

$$\mathcal{L}_Y = h_{ij}^d \bar{q}_L^i \phi_2 d_R^j + h_{ij}^u \bar{q}_L^i \tilde{\phi}_1 u_R^j + h_{ij}^e \bar{l}_L^i \phi_2 e_R^j + \text{H.c.}, \quad (2.2)$$

where the generic left-handed quark and lepton doublets are denoted by

$$q_L = \begin{pmatrix} u \\ d \end{pmatrix}_L$$

and

$$l_L = \begin{pmatrix} \nu \\ e \end{pmatrix}_L$$

and  $\tilde{\phi} = i\tau_2 \phi$  and  $i, j$  are family indices. Electroweak symmetry breaking is achieved by the vacuum expectation values (VEV's) of  $\phi_1$  and  $\phi_2$  given by

$$\langle \phi_1 \rangle = \frac{e^{i\theta}}{\sqrt{2}} \begin{pmatrix} 0 \\ v_1 \end{pmatrix} \quad (2.3)$$

and

$$\langle \phi_2 \rangle = \frac{1}{\sqrt{2}} \begin{pmatrix} 0 \\ v_2 \end{pmatrix}, \quad (2.4)$$

where the relative phase  $\theta$  between the two VEV's will be set to zero since we will not consider  $CP$  violation in this paper. The explicit representations of  $\phi_1, \phi_2$  are given as

$$\phi_1 = \begin{pmatrix} \phi_1^+ \\ \frac{1}{\sqrt{2}}(v_1 + R_1 + iI_1) \end{pmatrix}, \quad (2.5)$$

$$\phi_2 = \begin{pmatrix} \phi_2^+ \\ \frac{1}{\sqrt{2}}(v_2 + R_2 + iI_2) \end{pmatrix}.$$

After SSB, the following combination of Higgs fields

$$G^\pm = \frac{v_1 \phi_1^\pm + v_2 \phi_2^\pm}{v} \quad (2.6)$$

becomes the longitudinal mode of the physical  $W$  bosons leaving the charged-Higgs-boson pair as given by

$$H^\pm = \frac{v_2 \phi_1^\pm - v_1 \phi_2^\pm}{v}, \quad (2.7)$$

where  $v^2 = v_1^2 + v_2^2 = (246 \text{ GeV})^2$ . The  $W$ -boson mass is given by  $M_W = \frac{1}{2}gv$ . Similarly, the neutral would-be Goldstone boson

$$G^0 = \frac{1}{v}(v_1 I_1 + v_2 I_2) \quad (2.8)$$

becomes the longitudinal component of the  $Z$  boson. The three remaining neutral Higgs bosons will mix among

themselves. However, they do not enter into our discussions and henceforth will be ignored.

The same SSB also generates masses for the fermions via the Yukawa interactions of Eq. (2.2). Using Eqs. (2.2), (2.5), and (2.7) and diagonalizing the mass matrices of the quarks in the standard way, the  $H^\pm$  fermion-fermion couplings are then given by

$$\begin{aligned} L_Y^\pm = & \frac{\sqrt{2}}{v} \xi H^+ (\bar{u}, \bar{c}, \bar{t})_R M_U V \begin{pmatrix} d \\ s \\ b \end{pmatrix}_L \\ & + \frac{\sqrt{2}}{v} \frac{1}{\xi} H^+ (\bar{u}, \bar{c}, \bar{t})_L V M_D \begin{pmatrix} d \\ s \\ b \end{pmatrix}_R \\ & + \frac{\sqrt{2}}{v} \frac{1}{\xi} H^+ (\bar{\nu}_e, \bar{\nu}_\mu, \bar{\nu}_\tau)_L M_E \begin{pmatrix} e \\ \mu \\ \tau \end{pmatrix}_R + \text{H.c.}, \end{aligned} \quad (2.9)$$

where

$$\begin{aligned} M_U = & \begin{pmatrix} m_u & 0 \\ & m_c \\ 0 & m_t \end{pmatrix}, \quad M_D = \begin{pmatrix} m_d & 0 \\ & m_s \\ 0 & m_b \end{pmatrix}, \\ M_E = & \begin{pmatrix} m_e & 0 \\ & m_\mu \\ 0 & m_\tau \end{pmatrix}, \end{aligned} \quad (2.10)$$

and

$$V = \begin{pmatrix} V_{ud} & V_{us} & V_{ub} \\ V_{cd} & V_{cs} & V_{cb} \\ V_{td} & V_{ts} & V_{tb} \end{pmatrix}, \quad (2.11)$$

with  $V$  being the usual Kobayashi-Maskawa (KM) matrix.

Notice that the leptons do not have associated KM matrices as we keep the neutrinos massless. One other important coupling that we will use is the  $Z^\mu H^+ H^-$  vertex and this is given in Fig. 1. We denote the weak mixing angle by  $\theta_W$  and we shall use the value  $\sin^2 \theta_W = 0.22$ .

With the model detailed, the first step of our analysis is to calculate the mass difference  $\Delta M_B$  of  $B_d^0$  and  $\bar{B}_d^0$ . It is well known that charged Higgs bosons can lead to large  $\bar{B}^0 - B^0$  mixing.<sup>7</sup> The Feynman diagrams are depicted in Fig. 2 and they give<sup>7</sup>

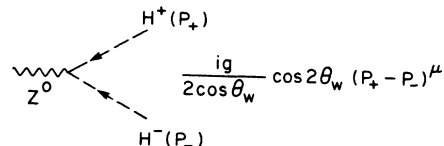


FIG. 1. Charged-Higgs-boson and  $Z$ -boson coupling.

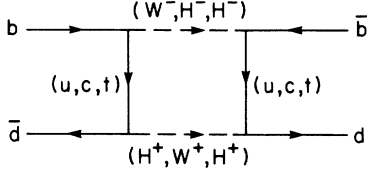


FIG. 2. Feynman diagrams involving charged-Higgs-boson contributions  $\Delta M_B$ .

$$\begin{aligned} \Delta M_B &= |M_{B_L} - M_{B_S}| \\ &= 2 |M_{12}| = \frac{f_B^2 B M_B V_{td}^{*2} V_{tb}^2 m_t^2}{48\pi^2 v^4} (I_{WW} + I_{WH} + I_{HH}), \end{aligned} \quad (2.12)$$

where

$$I_{WW} = 1 + \frac{9}{1-y_t^W} - \frac{6}{(1-y_t^W)^2} - \frac{6}{y_t^W} \left[ \frac{y_t^W}{1-y_t^W} \right]^3 \ln y_t^W, \quad (2.13)$$

$$I_{WH} = \xi^2 y_t^H \left[ \frac{(2x-8)\ln y_t^H}{(1-x)(1-y_t^H)^2} + \frac{6x \ln y_t^W}{(1-x)(1-y_t^W)^2} - \frac{8-2y_t^W}{(1-y_t^W)(1-y_t^H)} \right], \quad (2.14)$$

$$I_{HH} = \xi^4 y_t^H \left[ \frac{1+y_t^H}{(1-y_t^H)^2} + \frac{2y_t^H \ln y_t^H}{(1-y_t^H)^3} \right], \quad (2.15)$$

with  $y_i^\alpha = m(q_i)^2/M_\alpha^2$  ( $\alpha=W, H$ ) and  $x = M_H^2/M_W^2$ . The mass and the decay constant of the  $B$  meson are denoted by  $M_B$  and  $f_B$ , respectively. The values of these parameters are not well known. Different authors prefer very different values. We take the lowest values of  $M_B = 5.3$  GeV/ $c^2$ ,  $f_B = 0.16$  GeV, and  $B = \frac{1}{3}$ , which are the commonly used ones in the analysis of the kaon system.<sup>8</sup> We also compare the result with the largest values used in the literature:  $f_B = 0.20$  GeV and  $B = \frac{3}{2}$ . [The first set of parameters are used in Figs. 3(a) and 5(a)–7(a), and the second set are for Figs. 3(b) and 5(b)–7(b).] We also fix the KM elements to be given by  $|V_{td}| = 0.01$  and  $|V_{tb}| = 0.998$ . Thus, we consider  $\xi$ ,  $M_H$ , and  $m_t$  as the truly unknown parameters. Using the central value of the experimental measurement on  $\Delta M_B = 4 \times 10^{-13}$  GeV (Ref. 9), Eq. (2.12) gives a constraint on  $\xi$ ,  $M_H$ , and  $m_t$ . For a given  $\xi$  the allowed values of  $M_H$  and  $m_t$  are plotted in Fig. 3. We note that with these parameters the standard model will require  $m_t \simeq 300$  GeV/ $c^2$  in order to explain the magnitude of the observed  $B^0\text{-}\bar{B}^0$  mixing. Our analysis is an extension of Ref. 7 where it was pointed out that  $M_H = 25$  GeV/ $c^2$  and  $m_t \simeq 40$  GeV/ $c^2$  can account for “large”  $\Delta M_B$ . Clearly, the region of  $M_H < m_t$  is a very small one even with the hypothesis that the charged Higgs boson is important in  $B^0\text{-}\bar{B}^0$  mixing.<sup>10</sup> It seems much more likely that  $M_H > m_t$ . A look at Eqs. (2.13)–(2.15) reveals that charged-Higgs-boson effects dominate over the standard two  $W$ -boson exchange for values of  $\xi > 2$ . We show numerical results of up to

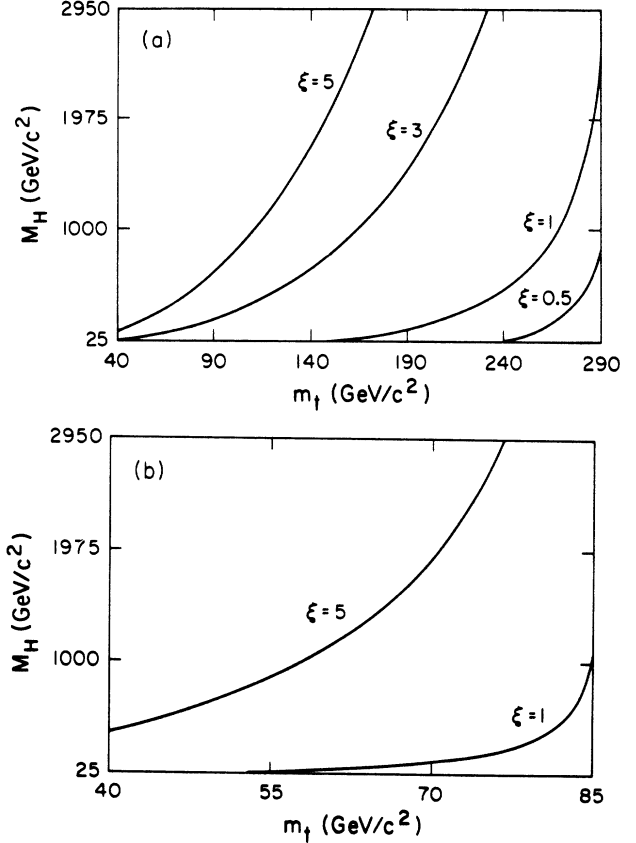


FIG. 3. Relation of  $M_H$  and  $m_t$  for different values of  $\xi$  with  $\Delta M_B = 4 \times 10^{-13}$  GeV in the minimal charged-Higgs-boson model. (a) is for  $f = 0.16$  GeV and  $B = \frac{1}{3}$  and (b) is for  $f = 0.2$  GeV and  $B = \frac{3}{2}$ .

$M_H = 2.95$  TeV/ $c^2$  and  $m_t = 290$  GeV/ $c^2$ . Considerations of perturbative unitarity<sup>11,12</sup> do not permit much larger values than these.

Here, we point out an interesting constraint on the Yukawa coupling  $h_t$  of the  $t$  quark coming from  $\Delta M_B$ . As is well known,  $h_t$  is related to the mass  $m_t$  via

$$\frac{h_t}{\sqrt{2}} = \frac{m_t}{v} (1 + \xi^2)^{1/2}. \quad (2.16)$$

In the MCH model one can take  $m_t$  and  $\xi$  as independent free parameters. The measurement of  $\Delta M_B$  now connects them together for a given  $M_H$ . In Table I we list the values of  $h_t$  calculated from Eqs. (2.12)–(2.15) and we can see that it varies very little with  $h_t/\sqrt{2} \simeq 1\text{--}2$ . This is surprisingly close to the value obtained from unitarity bound in SM (Ref. 11). In SM, with  $m_t \simeq 300$  GeV/ $c^2$ , it corresponds to  $h_t/\sqrt{2} \simeq 1.2$ .

With appropriate substitutions in the parameters of Eqs. (2.12)–(2.15), one can obtain  $\Delta M_K$ , the  $K_L^0, K_S^0$  mass difference. In this case the charm-quark exchange is the important term and charged-Higgs-boson effects are not significant.<sup>13</sup>

The virtual effects of the charged Higgs boson will also change the branching ratio of the rare decay  $K^+ \rightarrow \pi^+ \nu \bar{\nu}$  by interfering with the amplitudes of SM. The corre-

TABLE I. The Yukawa coupling of the  $t$  quark for different values of  $\xi$ ,  $M_H$ , and  $m_t$  in the MCH model as restricted by  $B_d^0\text{--}\bar{B}_d^0$  mixing.  $M_H$  denotes the charged-Higgs-boson mass in units of  $\text{GeV}/c^2$ .  $m_t$  denotes the  $t$ -quark mass in units of  $\text{GeV}/c^2$ .  $h'_i = h_i m_i / M_H$  is the reduced Yukawa coupling of the  $t$  quark.

| $\xi \backslash M_H$ | 900   |                        |                         | 500   |                        |                         | 300   |                        |                         | 100   |                        |                         |
|----------------------|-------|------------------------|-------------------------|-------|------------------------|-------------------------|-------|------------------------|-------------------------|-------|------------------------|-------------------------|
|                      | $m_t$ | $\frac{h_t}{\sqrt{2}}$ | $\frac{h_t'}{\sqrt{2}}$ | $m_t$ | $\frac{h_t}{\sqrt{2}}$ | $\frac{h_t'}{\sqrt{2}}$ | $m_t$ | $\frac{h_t}{\sqrt{2}}$ | $\frac{h_t'}{\sqrt{2}}$ | $m_t$ | $\frac{h_t}{\sqrt{2}}$ | $\frac{h_t'}{\sqrt{2}}$ |
| 1                    | 264.0 | 1.52                   | 0.45                    | 241.0 | 1.39                   | 0.67                    | 220.1 | 1.27                   | 0.93                    | 180.5 | 1.04                   | 1.88                    |
| 2                    | 202.9 | 1.84                   | 0.41                    | 169.5 | 1.54                   | 0.52                    | 143.2 | 1.30                   | 0.62                    | 100.2 | 0.91                   | 0.91                    |
| 3                    | 157.6 | 2.03                   | 0.36                    | 126.0 | 1.62                   | 0.41                    | 102.9 | 1.32                   | 0.45                    | 67.1  | 0.86                   | 0.58                    |
| 5                    | 105.9 | 2.20                   | 0.26                    | 81.0  | 1.70                   | 0.27                    | 64.9  | 1.35                   | 0.29                    | 40.0  | 0.83                   | 0.33                    |
| 8                    | 70.0  | 2.29                   | 0.18                    | 53.0  | 1.74                   | 0.18                    | 41.6  | 1.36                   | 0.19                    |       |                        |                         |
| 10                   | 56.9  | 2.33                   | 0.15                    | 42.9  | 1.75                   | 0.15                    |       |                        |                         |       |                        |                         |
| 14                   | 41.3  | 2.36                   | 0.11                    |       |                        |                         |       |                        |                         |       |                        |                         |

sponding Feynman diagrams are shown in Figs. 4(a)–(4c). The effective Lagrangian is calculated to be

$$y_j^\alpha = \frac{m(q_j)^2}{M_\alpha^2}, \quad z_i^\alpha = \frac{m(l_i)^2}{M_\alpha^2} \quad (\alpha = W, H),$$

$$\mathcal{L}_{\text{eff}}^{\bar{s}d \rightarrow \nu\bar{\nu}} = -\frac{g^2 V_{js}^* V_{jd}}{8\pi^2 v^2} D(y_j^\alpha, z_i^\alpha) (\bar{d} \gamma_\mu L s) (\bar{\nu} \gamma_\mu L \nu), \quad \text{and}$$

$$D = D_{\text{SM}} + D_{WH} + D_{HH} + D_{ZH},$$

$$\begin{aligned} D_{\text{SM}}(y^\alpha, z^\alpha) = & -\frac{1}{8} \frac{y^W z^W}{z^W - y^W} \left[ \frac{4 - z^W}{1 - z^W} \right]^2 \ln z^W + \frac{1}{4} y^W + \frac{3}{8} \left[ 1 - \frac{3}{1 - z^W} \right] \frac{y^W}{1 - y^W} \\ & + \frac{1}{8} \left[ \frac{y^W}{z^W - y^W} \left[ \frac{4 - y^W}{1 - y^W} \right]^2 + 1 + \frac{3}{(1 - y^W)^2} \right] y^W \ln y^W, \\ D_{WH}(y^\alpha, z^\alpha) = & y^W z^W \left[ \frac{y^W \ln y^W}{(1 - y^W)(z^W - y^W)(x - y^W)} + \frac{z^W \ln z^W}{(1 - z^W)(x - z^W)(y^W - z^W)} + \frac{x \ln x}{(1 - x)(z^W - x)(y^W - x)} \right. \\ & \left. + \frac{1}{4} \left[ \frac{x^2 \ln x}{(1 - x)(z^W - x)(y^W - x)} + \frac{(z^W)^2 \ln z^W}{(x - z^W)(1 - z^W)(y^W - z^W)} + \frac{(y^W)^2 \ln y^W}{(1 - y^W)(x - y^W)(z^W - y^W)} \right] \right], \end{aligned} \quad (2.17)$$

$$D_{HH}(y^\alpha, z^\alpha) = \frac{y^H z^H}{2g^2} \left[ \frac{1}{(1 - z^H)(1 - y^H)} - \frac{y^H \ln y^H}{(1 - y^H)^2 (z^H - y^H)} + \frac{z^H \ln z^H}{(1 - z^H)^2 (z^H - y^H)} \right],$$

$$D_{ZH}(y^\alpha, z) = \frac{-\xi^2 y^W}{4} \left[ \frac{y^H}{1 - y^H} + \frac{y^H \ln y^H}{(1 - y^H)^2} \right].$$

The branching ratio of  $K \rightarrow \pi \nu \bar{\nu}$  is given by

$$\begin{aligned} B(K^+ \rightarrow \pi^+ \nu \bar{\nu}) = & \frac{g^4}{128\pi^4} B(K^+ \rightarrow \pi^0 e^+ \nu_e) \sum_{i=1}^3 \frac{\left| \sum_{j=c,t} V_{js}^* V_{jd} D(y_j^\alpha, z_i^\alpha) \right|^2}{|V_{us}|^2} \\ = & 6.0 \times 10^{-7} \sum_{i=1}^3 \frac{\left| \sum_{j=c,t} V_{js}^* V_{jd} D(y_j^\alpha, z_i^\alpha) \right|^2}{|V_{us}|^2}. \end{aligned} \quad (2.18)$$

The SM contribution is given by  $D_{\text{SM}}$  (Refs. 14–16) whereas  $D_{WH}$  and  $D_{HH}$  denote box-diagram contributions involving one and two charged-Higgs-boson exchanges, respectively. They are negligible compared to

the next term represented by  $D_{ZH}$ . This is due to the fact that the box-diagram contribution involves the ratio  $m_l/v$  where  $l = e, \mu$ , and  $\tau$ , which is small. The  $\xi$ -factor enhancement is canceled. Our calculation of  $D_{ZH}$  gen-

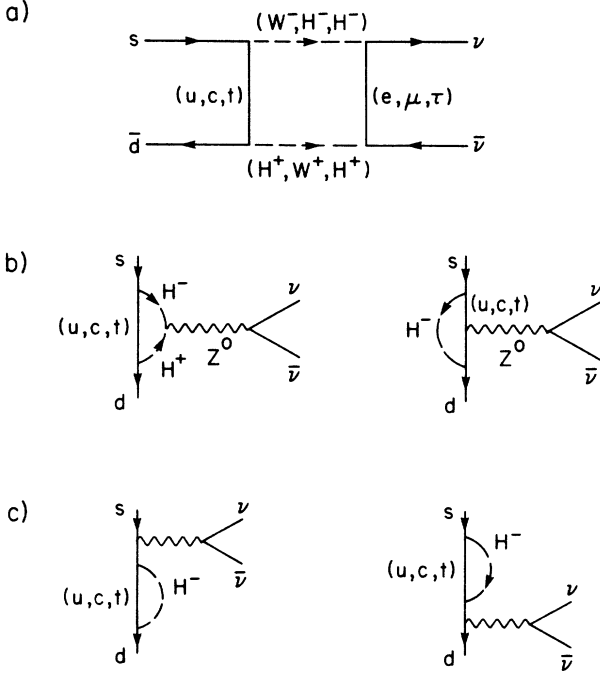


FIG. 4. Feynman diagrams with charged-Higgs-boson exchanges contributing to  $s \rightarrow d\nu\bar{\nu}$ .

eralizes that of Ref. 14. We find that the contribution for the charged Higgs boson interferes constructively with the SM amplitude, thereby enhancing the branching ratio. This enhancement increases with  $m_t$  but decreases with  $\xi$ . Also, it is not very sensitive to  $M_H$ . Naively, one expects an enhancement to increase like  $\xi^2$ . However, this is not the case because of the constraint from  $\Delta M_B$ . Large values of  $\xi$  are acceptable only if  $m_H$  is correspondingly large with relatively smaller values of  $m_t$  allowed. This gives the behavior of the branching ratio of reaction (1.2) plotted in Fig. 5 as a function of  $m_t$  for three fixed values of  $\xi$ . The value of the parameters used are those in calculated  $B_d^0\text{--}\bar{B}_d^0$  mixing. The mass  $M_H$  is not a free parameter but instead is given in Fig. 3. The insensitivity to  $M_H$  is due to the fact that for a given  $\xi$  the  $B^0\text{--}\bar{B}^0$  mixing forces  $M_H$  to increase much more rapidly than  $m_t$ , see Fig. 3, and  $D_{ZH}$  rapidly approaches its limiting value for large  $M_H$ . The maximum value of  $M_H$  for the curves of Fig. 5 is  $M_H = 2.95 \text{ TeV}/c^2$ . Values of  $\xi < 1$  are not very useful in achieving an enhancement of (1.1). Our calculations indicate that the MCH model gives at best a  $10^{-9}$  branching ratio for (1.1) for all reasonable values of  $\xi$ ,  $M_H$ , and  $m_t$ .

The physics that leads to charged-Higgs-boson enhancement in  $K \rightarrow \pi\nu\bar{\nu}$  decays is simply the property that it prefers to couple to the heaviest fermion around, which is the  $t$  quark in a six-quark world. Then we expect similar or even larger enhancement for reaction (1.2). The effective Lagrangian for  $b \rightarrow s\nu\bar{\nu}$  is given by Eq. (2.17) with changes of  $m_s$  to  $m_b$  and the KM matrix elements that dominate are  $V_{tb}$  and  $|V_{ts}| = 0.05$ .

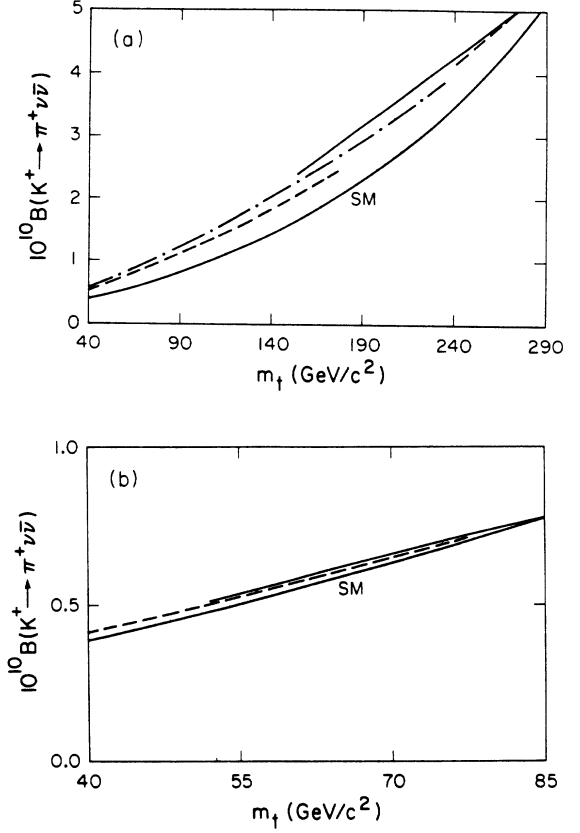


FIG. 5. Branching ratio of  $K \rightarrow \pi\nu\bar{\nu}$  as a function of  $m_t$  for fixed  $\xi$ . In (a) the standard-model result is given by the solid curve labeled SM. The upper curve is for  $\xi=1$ , the dashed-dotted curve is for  $\xi=3$ , and the lower dashed curve is for  $\xi=5$ . The upper dashed-dotted curve denotes  $\xi=0.5$ . In (b) the solid curve is for SM, the upper curve for  $\xi=1$ , and the dashed curve for  $\xi=3$ . (a) and (b) correspond to the different values of  $f$  and  $B$  as given by Figs. 3(a) and 3(b).

Straightforward calculations yield the branching ratio to be

$$B(b \rightarrow s\nu\bar{\nu}) = \frac{g^4}{256\pi^4} B(b \rightarrow (u, c)l\bar{\nu}_l) \times \sum_{i=1}^3 \frac{\left| \sum_{j=c,t} V_{js}^* V_{jb} D(y_j^\alpha, z_i^\alpha) \right|^2}{|V_{ub}|^2 + F(m_c^2/m_b^2) |V_{cb}|^2}. \quad (2.19)$$

Using  $B(b \rightarrow (u, c)l\bar{\nu}_l) = 0.12$ ,

$$B(b \rightarrow s\nu\bar{\nu}) = 7.5 \times 10^{-7} \frac{3 \left| \sum_{j=c,t} V_{js}^* V_{jb} D(y_j^\alpha, 0) \right|^2}{|V_{ub}|^2 + F(m_c^2/m_b^2) |V_{cb}|^2} \approx 22.5 \times 10^{-7} \frac{|D(y_t^\alpha, 0)|^2}{F(m_c^2/m_b^2)}, \quad (2.20)$$

where  $F(m_c^2/m_b^2) \approx 0.5$  is a phase-space factor. As a comparison, the inclusive decay  $B \rightarrow X_s \nu\bar{\nu}$  is plotted in

the same manner as the decay (1.1).

The abrupt beginning and ending of the curves in Figs. 3, 5, and 6 are due to the cutoff that we imposed: namely,  $m_t < 290 \text{ GeV}/c^2$  and  $M_H < 2.95 \text{ TeV}/c^2$  as read from Fig. 3. Clearly, the MCH predicts very similar enhancement over SM for both (1.1) and (1.2).

Reaction (1.2) suffers from being very difficult to measure at best, even at a dedicated  $B$ -meson factory. On the other hand, the rare decay of  $b \rightarrow s\gamma$  with a hard photon is easier since one can directly measure the hard photon but not the neutrinos. The branching ratio with charged-Higgs-boson effects<sup>5</sup> is known in the literature and we shall not repeat them here. Using our parameters and constraint from  $B_d^0 - \bar{B}_d^0$  mixing as presented in Fig. 3, we calculated the branching ratio  $(b \rightarrow s\gamma)/(b \rightarrow sl\bar{\nu}_l)$ , and this is plotted in Fig. 7. An examination of this shows that again an enhancement over the SM results is obtained. As contrary to (1.1) and (1.2), the region where the branching ratio is most enhanced comes from smaller values of  $m_t$ . The branching ratio falls as a function of  $m_t$ . In this decay SM plays a more important role. The MCH model value is rapidly approaching that of the SM prediction as  $m_t$  increases.

Before we draw our conclusions we give a comparison with the works of Ref. 5 which studied charged-Higgs-boson effects in  $B$ -meson decays. Both papers of Ref. 5 overlap with ours in the calculation of  $\Delta M_B$  and the reaction (1.3). Our results for (1.3) cover the full range of

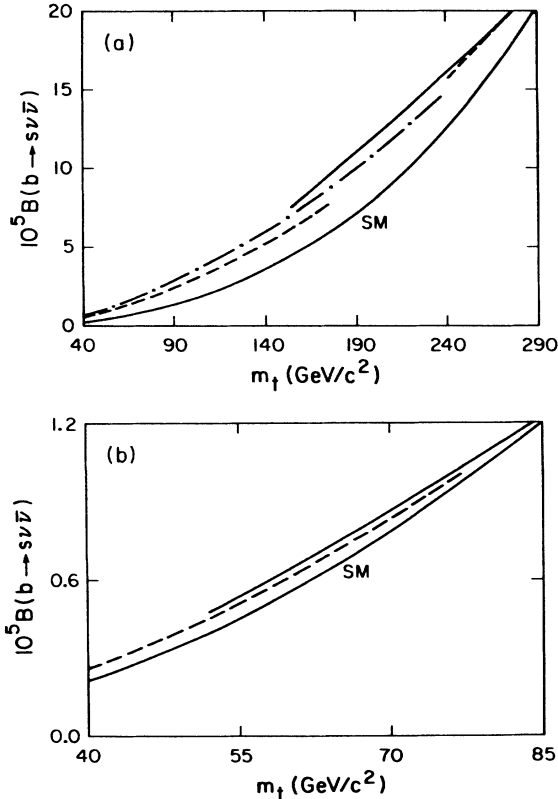


FIG. 6. Branching ratio of  $b \rightarrow s\nu\bar{\nu}$  to all as a function of  $m_t$  for fixed  $\xi$ . Labels of the curves are the same as in Fig. 5.

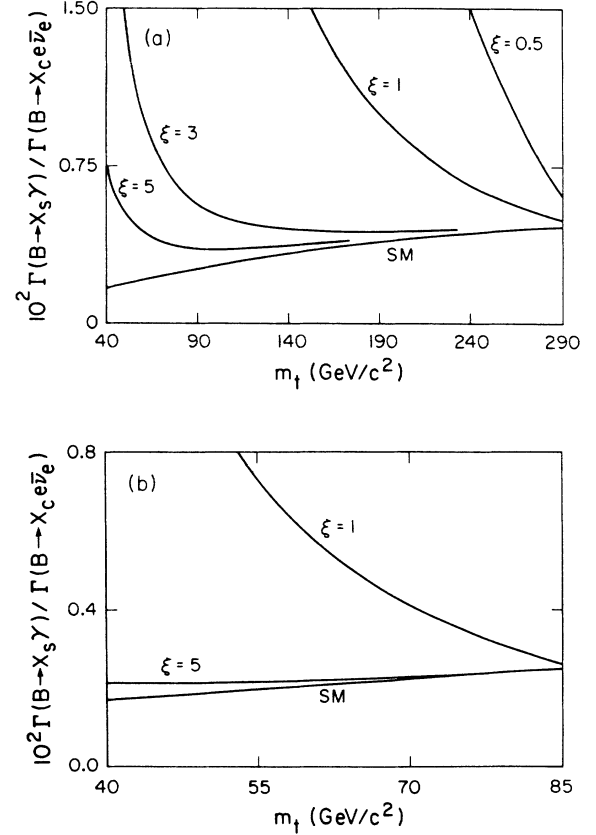


FIG. 7. The width of  $b \rightarrow s\gamma$  vs  $b \rightarrow sl\bar{\nu}_e$  as a function of  $m_t$  for fixed  $\xi$ . The curves are labeled as in Fig. 5.

values in  $m_t$  and  $M_H$  as allowed by  $\Delta M_B$ , whereas Grinstein and Wise give only the result for  $m_t = 50 \text{ GeV}/c^2$  and  $M_H \leq 150 \text{ GeV}/c^2$ . We agree with their results where the parameters overlap. While QCD corrections are included in our calculation of (1.3), Hou and Willey have not included them. Furthermore, both papers in Ref. 5 did not consider  $K \rightarrow \pi\nu\bar{\nu}$  and  $B \rightarrow X_s\nu\bar{\nu}$  decays.

### III. CONCLUSIONS

We have calculated the effects of charged Higgs bosons on the rare decay (1.1) by using the constraint observed from  $\Delta M_B$ . This is predicated upon the optimistic assumption that the observed “large”  $B^0 - \bar{B}^0$  mixing signals the possible existence of  $H^\pm$ . We hasten to add that this need not be the case. By using different parameters<sup>16,17</sup> one can also explain  $\Delta M_B$  with  $m_t > 50 \text{ GeV}/c^2$  without having to invoke the existence of charged Higgs bosons. Clearly, finding the  $t$  quark is very important although this does not rule out the existence of  $H^\pm$ . In these events the constraint of Eq. (2.12) becomes more restrictive. We note in passing that for  $H^\pm$  to be important in  $\Delta M_B$ , the preferred values of  $\xi$  are greater than unity and a  $t$  quark should not be overly heavy.<sup>18</sup> Surprisingly, the Yukawa coupling is always of the order of unity.

Charged Higgs bosons make considerable contributions to the rare decay (1.1) and (1.2). For the  $K \rightarrow \pi\nu\bar{\nu}$

decay a branching ratio of  $10^{-9}$  will indicate a  $\xi \simeq 1$  value with  $m_t \simeq 290$  GeV/ $c^2$ . A factor of approximately 1.5 enhancement over the standard-model result can be achieved. However, a branching ratio of  $10^{-8}$  cannot be obtained with the MCH model, as we have analyzed. Changing the parameters  $f_B$  and  $B$  will not push the branching up. This is clearly seen by comparing the sets of graphs labeled (a) and (b). In the event that a branching ratio  $\sim 10^{-8}$  is measured, then the corresponding new physics is beyond the conservative MCH model we studied and certainly beyond SM. On the other hand, the decay of the  $B$  meson with a hard photon in the final state is also enhanced and a branching ratio  $\sim 10^{-3}$  is predicted, albeit with different values of  $m_t$  and  $\xi$ .

We have illustrated the use of rare decays of  $B$  mesons and the kaon as a probe of the physics of charged Higgs bosons. For example, if a branching ratio of  $(1.1) \sim 10^{-9}$  is found and  $m_t$  is found not to be near 290 GeV/ $c^2$ , then it will again rule out the MCH model as the sole source of new physics. Then we must add even more structure to the standard model. On the other hand, if its measurement is below the minimum predicted by SM it will also rule out the charged Higgs boson playing a role in these decays. Since  $H^\pm$  adds to the SM amplitudes the branching ratio of (1.1) is always enhanced. Unfortunately, to

reach a branching ratio of  $\sim 10^{-10}$  is beyond the present experimental capability. Because of the important impact they may have in revealing new physics, all three reactions (1.1)–(1.3) should be pushed to the limit we have indicated.

*Note added.* Recently, an improved measurement of  $B \rightarrow K^* \gamma$  has been reported by the CLEO group at the Snowmass Conference. The upper limit of the branching ratio is  $1.7 \times 10^{-4}$ , from which we can infer the inclusive branching ratio

$$(b \rightarrow s \gamma)/(b \rightarrow \text{all}) \leq (2.4\text{--}3.8) \times 10^{-3}.$$

At present it does not rule out the MCH model. An order-of-magnitude improvement will rule out small values of  $m_t$  and  $m_H$ , such as  $m_t \leq 100$  and  $m_H \leq 100$  GeV/ $c^2$  for  $f_B B = 160$  MeV. This will also limit the allowed values of  $m_t \leq 100$  GeV/ $c^2$  in the standard model with QCD corrections included.

#### ACKNOWLEDGMENTS

This work was supported in part by the Natural Sciences and Engineering Council of Canada. We would like to thank Dr. R. D. Peccei for many useful conversations.

<sup>1</sup>For reviews, see J. E. Kim, Phys. Rep. **150**, 1 (1987); H. Y. Cheng, *ibid.* **158**, 1 (1988).

<sup>2</sup>R. D. Peccei and H. R. Quinn, Phys. Rev. Lett. **38**, 1440 (1977); Phys. Rev. D **16**, 1791 (1977).

<sup>3</sup>J. F. Gunion, G. L. Kane, and J. Wudka, Nucl. Phys. **B289**, 231 (1988).

<sup>4</sup>Brookhaven National Laboratory Experiment No. E-787.

<sup>5</sup>B. Grinstein and M. B. Wise, Phys. Lett. B **201**, 274 (1988); W. S. Hou and R. S. Willey, *ibid.* **202**, 591 (1988).

<sup>6</sup>For a review, see R. A. Flora and M. Sher, Ann. Phys. (N.Y.) **148**, 95 (1983).

<sup>7</sup>S. L. Glashow and E. E. Jenkins, Phys. Lett. B **196**, 233 (1987).

<sup>8</sup>The parameter  $B$  denotes the ratio of the actual hadronic matrix element to its vacuum-insertion value. Its value ranges from  $\frac{1}{3}$  to  $\frac{3}{2}$ .

<sup>9</sup>Argus Collaboration, H. Albrecht *et al.*, Phys. Lett. B **192**, 245 (1987).

<sup>10</sup>Our numerical results agree with that of Ref. 7 when we use their parameters.

<sup>11</sup>M. S. Chanowitz, M. A. Furman, and I. Hinchliffe, Nucl. Phys. **B153**, 402 (1979).

<sup>12</sup>H. Hufel and G. Pocsik, Z. Phys. C **8**, 13 (1981); R. Casalbuoni, D. Dominici, R. Gatto, and C. Giunti, Phys. Lett. **78B**, 235 (1986).

<sup>13</sup>The constraint  $m_c$ ,  $m_H$ , and  $\xi$  is automatically satisfied. This is not as tight a constraint as given by  $\Delta M_B$ . L. F. Abbott, P. Sikivie, and M. B. Wise, Phys. Rev. D **21**, 1393 (1980).

<sup>14</sup>T. Inami and C. S. Lim, Prog. Theor. Phys. **65**, 297 (1981).

<sup>15</sup>W. S. Hou, R. S. Willey, and A. Soni, Phys. Rev. Lett. **58**, 1608 (1987).

<sup>16</sup>J. Ellis, J. S. Hagelin, and S. Rudaz, Phys. Lett. B **192**, 201 (1987); H. Harari, and Y. Nir, *ibid.* **195**, 586 (1987).

<sup>17</sup>I. I. Y. Bigi and A. I. Sanda, Phys. Lett. B **194**, 307 (1987); L. Chau and W. Y. Keung, University of California at Davis Report No. UCD-87-02 (unpublished); V. Barger, T. Han, D. V. Nanopoulos, and R. T. N. Phillips, Phys. Lett. B **194**, 312 (1987); D. Du and Z. Zhao, Phys. Rev. Lett. **59**, 1072 (1987); J. F. Donoghue *et al.*, Phys. Lett. B **195**, 285 (1987); W. Hou and A. Soni, *ibid.* **196**, 92 (1987); J. R. Cudell, F. Halzen, X. G. He, and S. Pakvasa, *ibid.* **196**, 227 (1987).

<sup>18</sup>The features we have discussed hold true for the whole range of  $\Delta M_B$  of  $(3\text{--}5) \times 10^{-13}$  GeV.